Remote Triggered Release of Doxorubicin in Tumors by Synergistic Application of Thermosensitive Liposomes and Gold Nanorods

Abhiruchi Agarwal,[†] Megan A. Mackey,[‡] Mostafa A. El-Sayed,[‡] and Ravi V. Bellamkonda[†,*]

[†]Neurological Biomaterials and Cancer Therapeutics Laboratory, Wallace H Coulter Department of Biomedical Engineering, Georgia Institute of Technology, Atlanta, Georgia 30332, United States, and [‡]Laser Dynamics Laboratory, School of Chemistry and Biochemistry, Georgia Institute of Technology, Atlanta, Georgia 30332, United States

ABSTRACT Delivery of chemotherapeutic agents after encapsulation in nanocarriers such as liposomes diminishes side-effects, as PEGylated nanocarrier pharmacokinetics decrease dosing to healthy tissues and accumulate in tumors due to the enhanced permeability and retention effect. Once in the tumor, however, dosing of the chemotherapeutic to tumor cells is limited potentially by the rate of release from the carriers and the size-constrained, poor diffusivity of nanocarriers in tumor interstitium. Here, we report the design and fabrication of a thermosensitive liposomal nanocarrier that maintains its encapsulation stability with a high concentration of doxorubicin payload, thereby minimizing "leak" and attendant toxicity. When used synergistically with PEGylated gold nanorods and near-infrared stimulation, remote triggered release of doxorubicin from thermosensitive liposomes was achieved in a mouse tumor model of human glioblastoma (U87), resulting in a significant increase in efficacy when compared to nontriggered or nonthermosensitive PEGylated liposomes. This enhancement in efficacy is attributed to increase in tumor-site apoptosis, as was evident from noninvasive apoptosis imaging using Annexin-Vivo 750 probe. This strategy affords remotely triggered control of tumor dosing of nanocarrier-encapsulated doxorubicin without sacrificing the ability to differentially dose drugs to tumors *via* the enhanced permeation and retention effect.

KEYWORDS: triggered drug release · nanocarrier · glioma · cancer · nanotechnology

PEGylated nanocarriers can evade the reticulo-endothelial system (RES) and deliver high payloads of encapsulated drug molecules at the tumor site compared to healthy tissue[1,2] due to enhanced permeation and retention (EPR) effect.[3] However, once extravasated, nanocarriers accumulate close to the blood vessels and further tissue diffusion is limited due to their relatively large size compared to the drugs they encapsulate.[4] In addition, the release of the drug from these nanocarriers is not controlled and is relatively slow.[5] Several triggered release systems have been fabricated with triggers such as pH,[6,7] light,[8,9] enzymes,[10,11] and heat[12−15] in an attempt to improve drug bioavailability to the tumor interstitium. However, the stability of such systems in the systemic circulation remains a challenge,[16] compromising the inherent advantages of nanocarriers to protect the drug, prevent promiscuous delivery to nontarget tissues, and limit systemic toxicity. Therefore, maintaining drug encapsulation stability while in circulation while still enabling reproducible and controlled remote triggered release from nanocarriers in tumors remains a challenge.

Recently, photothermal hyperthermia in tumors mediated by near-infrared (NIR) radiation of plasmonic nanoparticles that exhibit strong absorption in the visible as well as NIR regions due to surface plasmon resonance oscillations has been reported.[17−20] Due to minimal attenuation by water and hemoglobin, NIR in the 650−900 nm range is advantageous, and NIR transmission in soft tissues may be achieved at depths up to 10 cm.[21,22] Gold nanorods (GNRs) are particularly attractive, as their dimensions can be tuned to absorb in the NIR region, enabling heating localized to GNR location. Interestingly, GNRs accumulate specifically in tumor tissue due to EPR effect.[23] By optimizing variables that include shape, size, and amount of the GNRs coupled with NIR field strength, precise and localized control over tumor tissue heating can potentially be achieved.

Here, we report the fabrication of improved and relatively stable 100 nm thermosensitive liposomes. We employed GNRs to synergistically, noninvasively, and spatially trigger the release of the chemotherapeutic doxorubicin from the thermosensitive liposomes after their passive accumulation in a U87 human glioma model. In doing so, we

* Address correspondence to ravi@gatech.edu.

Received for review March 16, 2011 and accepted May 19, 2011.

Published online May 19, 2011
10.1021/nn201010q

TABLE 1. Comparison of Encapsulated DXR Release from Different Liposomes to NTSL, after 24 h incubation at 37 °C (column 1)[a]

	% DXR released	
	24 h, 37 °C	10 min, 43 °C
97−x% DPPC/x% Chol/3% PEG		
x		
0	56 ± 4[c]	NA
15	50.57 ± 1.73[c]	NA
25	22.57 ± 1.08[c]	Δ 4.07 ± 4.26
30	12.78 ± 2.08	Δ 1.07 ± 1
97−x% DSPC/x% DPPC/3% PEG		
x		
0	2.07 ± 0.35[c]	NA
15	10.28 ± 2.83	Δ 6.16 ± 3.85
25	7.93 ± 1.26	Δ 5.70 ± 0.39
40	19.04 ± 2.83[b]	Δ 5.03 ± 3.23

[a] Samples were then placed for 10 min at 43 °C (column 2). Data reported are mean ± SD ($n = 4$). [b] $p < 0.01$. [c] $p < 0.001$ compared to NTSL.

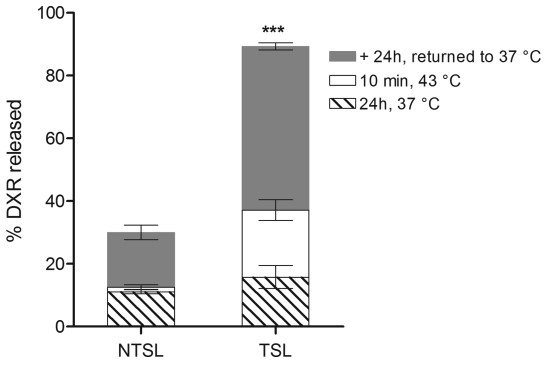

Figure 1. Release of DXR from liposomes. DXR released after 24 h at 37 °C (diagonal stripes) was quantified from thermosensitive liposomes, TSL (DPPC/Chol/DMPC/PEG), and non-thermosensitive liposomes, NTSL (HSPC/Chol/PEG). After 24 h at 37 °C, liposomes were transferred to a higher temperature of 43 °C for 10 min, and DXR release was quantified, indicated by □. TSL showed comparable stability after a 24 h period at 37 °C to NTSL and was able to show significant amount of DXR release upon heating to 43 °C (*$p < 0.001$). After heating at 43 °C for 10 min, liposomal formulations were transferred back to 37 °C water bath and their release was quantified after another 24 h, indicated by ■. NTSL still carried DXR very stably. In contrast, TSL formulation lost ∼90% of the drug ($n = 4$).**

achieved enhanced control over drug release at the desired site. The synergistic application of GNRs with thermosensitive liposomes led to significantly enhanced therapeutic efficacy.

RESULTS AND DISCUSSION

Encapsulation Stability and Thermosensitive Release of Chemotherapeutic Doxorubicin from Liposomal Nanocarriers. Thermosensitive liposomes previously reported in the literature are unstable and experience extensive drug loss from the nanocarriers at physiological temperature in contrast to FDA-approved liposomal doxorubicin composed of HSPC/Chol/PEG, 100:30:6 (NTSL, non-thermosensitive stealth liposomes). Loss of drug at physiological temperature compromises passive drug accumulation in the tumor and increases systemic cytotoxicity. Several liposomal formulations encapsulating doxorubicin (DXR) were fabricated with and tested for drug encapsulation stability at physiological temperature and release at 4−5 °C elevated temperature. All liposomal formulations were sized 120 ± 10 nm, as confirmed by dynamic light scattering (data not shown). DPPC liposomes, devoid of any cholesterol, rendered the liposomes highly unstable, and liposomes did not carry the drug stably over extended periods of time at physiological temperatures (Table 1). In 24 h, DPPC liposomes lost more than 50% of the encapsulated DXR. DSPC (1,2-distearoyl-*sn*-glycerophosphocholine) liposomes, on the other hand, do not release any DXR at 37 °C, which can be attributed to their very high transition temperature of 55 °C, preventing ripple phase and, therefore, leakiness. By adding increasing amounts of DPPC to DSPC liposomes (≥40% DPPC) a significant increase in the release of DXR was assessed in comparison to NTSLs (Table 1). No significant increase in DXR release was seen from these formulations upon heating at 43 °C. DXR, upon remote loading, is trapped inside the liposomes as precipitates of the sulfate. The slight increase in release of DXR upon heating to 43 °C, for all liposomes containing varying amounts of DPPC, could be due to increase in DXR solubility in comparison to its solubility at 37 °C and increase in lipid kinetic energy, leading to thinning of the liposomal membrane. Increase in DXR solubility and loss of protons due to increase in the bilayer permeability may enable outward movement of DXR amphiphile recorded as released DXR. Therefore, the thermosensitive nanocarriers' liposomal membrane composition needs to be optimized for the chemotherapeutic drug of choice. DPPC liposomes were also fabricated by inclusion of varying amounts of cholesterol. It was found that 30% cholesterol in DPPC liposomes results in a very small loss of DXR over a 24 h period at 37 °C (Table 1). However, these liposomes, also, do not exhibit any thermosensitivity at 43 °C, which is higher than DPPC phase transition. Cholesterol, therefore, has a stabilizing effect on the DPPC membrane, as shown here and in earlier reports.[24] We, therefore, investigated the inclusion of small amounts of a low transition temperature (23 °C) lipid DMPC on the stability and thermosensitivity of the liposomes. As shown in Figure 1, inclusion of 30% cholesterol and small amounts (3%) of DMPC resulted in a liposome (DPPC/Chol/DMPC/PEG, 54:30:3:3, thermosensitive stealth liposomes, TSLs) that would carry its content stably at physiological temperature and released DXR at 43 °C when heated for 10 min. Reduction of cholesterol to 25% or inclusion of DMPC at 7% in these liposomes reduced their stability at 37 °C. Heating for 10 min and placing TSLs back in 37 °C for an additional

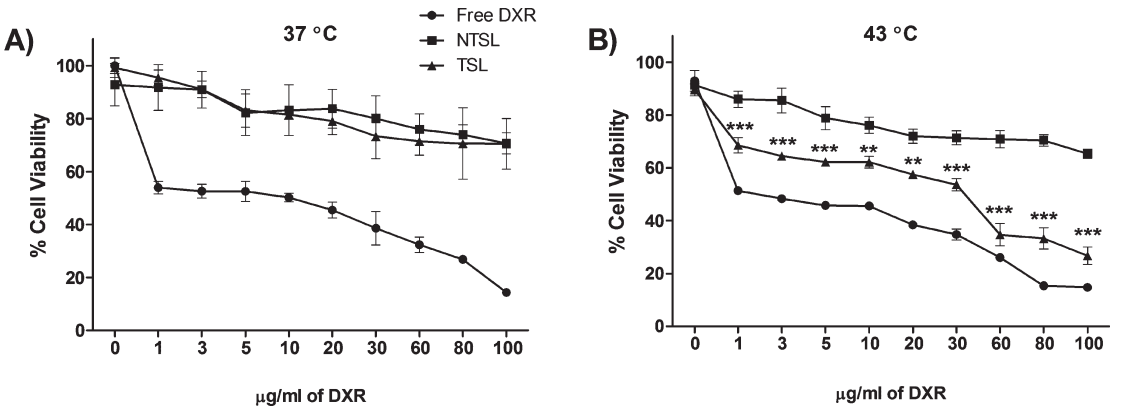

Figure 2. ***In vitro*** **heat-mediated cell cytotoxicity of liposomal formulation. Cells were treated with free DXR, non-thermosensitive liposomes (NTSL), or thermosensitive liposomes (TSL) with varying DXR concentrations at (A) 37 °C or (B) 43 °C. Cell cytotoxicity was measured by modified MTT assay (CCK8). Cells treated with TSL showed significant increase in cytotoxicity at 43 °C in comparison to NTSL (**$p < 0.01$ or ***$p < 0.001$) at all DXR concentrations. TSLs were significantly cytotoxic at 43 °C in comparison to those at 37 °C ($p < 0.001$). Data represented are mean ± SD ($n = 4$).**

24 h resulted in ~90% release of DXR from these liposomes (Figure 1). In contrast, NTSLs show only a modest release of ~40% total DXR content. Fast release of the chemotherapeutic can result in better bioavailability of the drug and higher apoptosis rate, as is explained later in this report. In our study, TSL showed maximum release at 43 °C when tested for drug release at the temperature range of 37−45 °C. The ceiling of this range of 43 °C was chosen, as one of the design criteria is to minimize focal temperature highs in the brain while maximizing release from TSLs to ensure safety. Hence the optimization was to achieve a temperature where the enhanced release was significant, temperature increases were minimal, and the time to attain the temperature of interest (in this case 43 °C) was reasonable from a clinical perspective (10 min in our study).

In Vitro **Cytotoxicity Studies.** Cytotoxicity of TSL formulation was determined by evaluating cell viability to ensure that the extent of DXR release at 43 °C was cytotoxic in comparison to NTSL (Figure 2). Untreated cells were unaffected by temperature change, with the viability of cells being at 100%. Cells exposed to empty liposomes (NTSLs or TSLs) also did not show change in viability at either temperature. Cell viability remained unaffected upon treatments with NTSLs, did not show any significant change due to change in temperature, and exhibited approximately 70−90% viability under all conditions (Figure 2). TSLs, however, demonstrated a significant increase in cytotoxicity over NTSLs at 43 °C ($p < 0.001$) at all DXR concentrations, confirming the release of DXR from TSLs and, thereby, the cytotoxic effect at higher temperature. Free DXR depicted an LC_{50} at 10 μg/mL DXR concentration. TSLs did not show an increase in cytotoxicity at 37 °C, and the results were comparable to cells treated with NTSLs. However, at 43 °C TSLs showed an LC_{50} between 30 and 60 μg/mL.

In Vivo **Drug Studies.** Further, to assess the cytotoxic effect and therapeutic efficacy of the TSLs triggered *via* GNRs in NIR, we used a xenograft mouse model of human glioma U87-MG. U87-MG is known to form sizable and repeatable tumors in nude mice and therefore were suitable for this study.[25,26] In this study, we co-injected the liposomal drug and GNRs and waited 48 h to apply NIR. In doing so, we assess the capability of the GNRs in disrupting the liposomes *in vivo*, as well as compare the effect of burst release of the drug from the nanaocarriers to drug being released from non-disruptable nanocarriers for long periods of time after passive accumulation. Animals received liposomal DXR or saline ± GNR (Figure 3A) when the tumor size was ~4−6 mm. The average temperature increase was assessed and recorded using a 33-gauge hypodermic thermocouple (Omega), 10 mm long. The measured temperature of all animal tumors receiving 5 pmol/kg of GNRs (810 nm; 0.5 W/cm^2) irradiated with NIR was 43 ± 1 °C. All animal tumors that did not receive GNRs but were irradiated with NIR recorded an average temperature of 39 ± 1 °C. The basal temperature of tumors before NIR irradiation was 34−35 °C primarily due to loss of heat as animals were anesthetized for NIR irradiation. Injecting a larger dose of GNRs resulted in tumor temperatures > 45 °C. Therefore, the 5 pmol/kg GNR dose was used in these studies.

GNR-mediated heating of TSL was highly effective in suppressing tumor progression. As seen in Figure 3B, animals that received a single combination treatment of TSL + GNR + NIR did not show an increase in the size of tumors for up to 21 days. All saline-treated animals, in contrast, showed an exponential increase in tumor size. All other liposomal treatments with or without GNR/NIR were also able to suppress tumors, on average, for up to 17 days. There was a significant difference in the ability to suppress tumors overall between TSL + GNR + NIR treatment and all other treatments

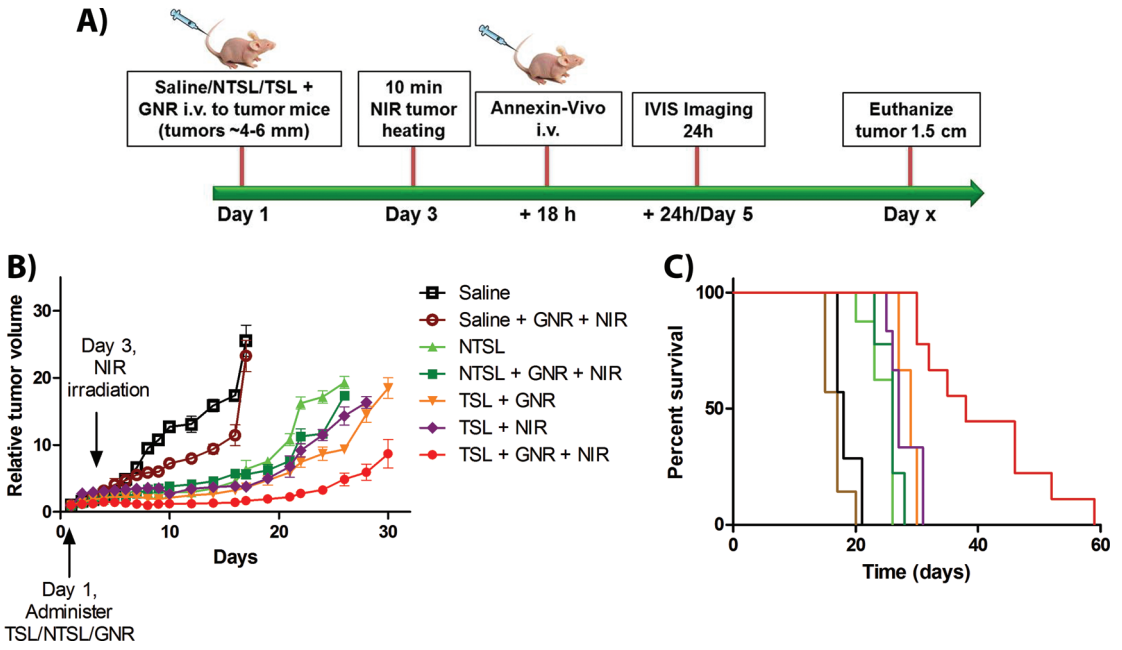

Figure 3. Therapeutic efficacy. Nude mice were injected with 2×10^6 U87-MG. (A) Schematic of treatment administration and *in vivo* imaging. (B) Relative tumor volume after treatment administration in different groups ($n = \sim 6-9$) was measured every day for the first 10 days and every other day after day 10. Mice received either liposomal DXR (2.5 mg/kg) or saline in combination with GNRs at 5 pmol/kg of rods; 48 h later, mice received NIR irradiation with a laser (808 nm, 0.5 W/cm^2) for 10 min. TSL + GNR + NIR were significantly different from the saline groups (day 6−17, $p < 0.001$). Animals that were treated with TSL + GNR + NIR were significantly different from all other liposomal treatment groups (day 19−26, $p < 0.001$). Data represented are mean ± SEM. (C) Percent survival for different treatment groups ($n = \sim 6-9$). Mantel−Cox analysis indicated that TSL + GNR + TSL was significantly different from all other groups ($p < 0.0001$).

($p < 0.001$). In addition, TSL + GNR + NIR treatment was successful in extending overall survival (median survival = 38 days, a 31% improvement over all other groups, Figure 3C). In contrast, saline-treated animals ± GNR-mediated heating did not show such pronounced effects, with median survival of 17 days. Animals that received either NTSL ± GNR-mediated heating or TSL ± NIR were also less successful in prolonging survival in comparison to TSL + GNR + NIR treatment. All animals receiving liposomal DXR at 2.5 mg/kg showed significant tumor suppression in comparison to saline-treated animals with or without GNR-mediated heating. In our studies, we tested 10 and 5 mg/kg DXR doses as well; however, animals did not tolerate these doses very well and were not further investigated.

Increased animal survival indicated that GNR-mediated heating results in increased bioavailability of DXR trapped in TSLs. The incapability of NTSL + GNR + NIR, or NR + NIR, to significantly affect tumor progression demonstrates that the therapeutic effect observed is DXR mediated and was not due to the 4−5 °C elevation of tumor temperatures. Therefore, GNRs can be effectively used to remotely and locally trigger the release of the drug from nanocarriers, thereby promoting drug bioavailability. Remote triggered release of liposomal content *via* GNRs was demonstrated previously[27,28] by incorporating the gold nanoparticles inside the liposomes. However, the liposomes fabricated in these studies were large (>200 nm), due to encapsulation of gold particles inside the liposomes, which compromises their circulation times and passive tumor accumulation. In addition, the encapsulation stability of these liposomes over a 24 h period was not demonstrated, and this is a critical design requirement for nanocarrier-encapsulated chemotherapeutic delivery, as it directly impacts systemic toxicity and side-effects. In our current study, we demonstrated the synergistic combination of plasma stable liposomes with co-accumulated GNRs can be used to stimulate the fast release of chemotherapeutic drug to achieve cytotoxicity.

Apoptosis Imaging. To demonstrate the immediate effect of drug release from the nanocarriers on cell viability *in vivo*, we used Annexin-Vivo 750.[29] Annexin injected 18 h after NIR irradiation was able to bind to apoptotic cells and reveal information about immediate cell death induced by drug release.

In vivo fluorescence imaging provides inexpensive and rapid assessment of real-time biological processes[30,31] in contrast to MRI or histological techniques. To assess the short-term effect of various drug treatments, we measured and quantified the extent of apoptosis at the tumor site using an *in vivo* fluorescence modality. Apoptotic agent Annexin-Vivo (excited at 740; emission collected at 780 nm) was administered 18 h after the tumors were heated *via* NIR (see Figure 3A). Imaging was conducted at 24 h post-annexin

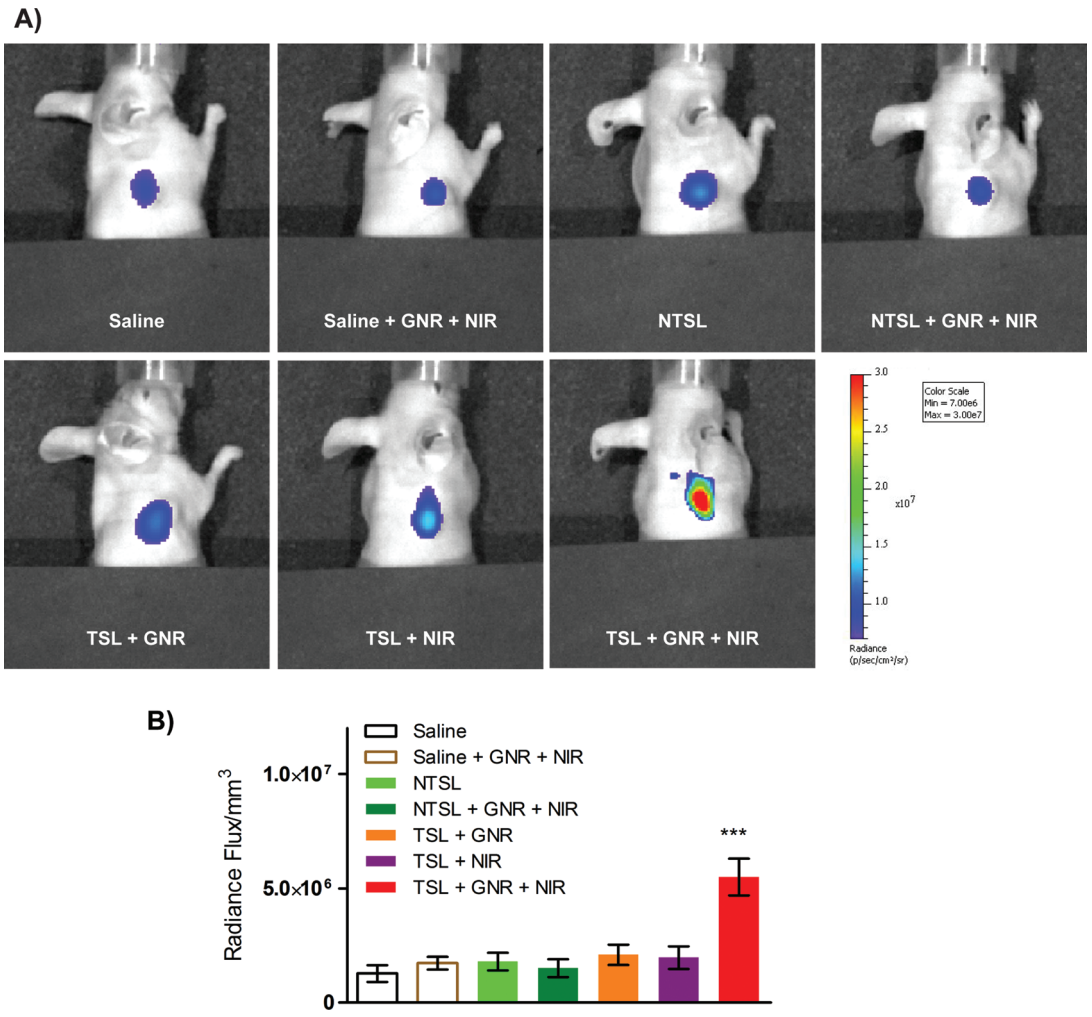

Figure 4. ***In vivo*** **apoptosis imaging shows higher accumulation and retention of apoptosis marker Annexin-Vivo 750. (A) Representative** ***in vivo*** **images 24 h after Annexin-Vivo administration for different treatment groups as indicated. (B) Different groups of tumor-bearing animals, 18 h post-NIR irradiation, were administered Annexin-Vivo 750 i.v. and were imaged 24 h later. Fluorescence intensity acquired in photons/s was quantified by drawing a region of interest around the tumor. The resulting radiance flux was then normalized by each animal's tumor volume measured using calipers. Animals treated with TSL + GNR + NIR were significantly different from all other groups (*** $p < 0.0001$, ANOVA).**

administration, and the fluorescent signal was quantified for each animal and normalized by their respective tumor volume determined *via* calipers to obtain a per cell apoptosis intensity. Enhancement in signal intensity can be attributed to an increase in annexin binding at the tumor site. At 24 h, the TSL + GNR + NIR group showed the maximum radiance flux per cubic millimeter, indicating retention of annexin at the tumor after clearance of annexin from the blood pool (Figure 4). Annexin clearance could be easily detected through the kidneys as the fluorescence recorded in this area was much higher than the tumor. As a result, the charged couple device (CCD) was flooded with photons from the kidney area and could not detect differences in the tumor apoptosis in uncovered animals. Therefore, animals had to be covered with a black paper to cover the kidneys and reveal the differences in the annexin accumulation in the tumors.

Apoptosis imaging can be used as a powerful tool to assess the success of a treatment in suppressing tumors.

CONCLUSION

When fabricating nanocarriers for triggered release of contents at desired tumor sites, two problems are often difficult to overcome: (1) making a stable triggerable formulation that does not leak while in systemic circulation and (2) a precise, externally controlled remote trigger.[32]

In this report we designed a thermosensitive liposomal nanocarrier that can stably hold DXR in the plasma over a period of 24 h and release its contents when heated at 43 °C. Co-delivery of GNRs with liposomes and application of NIR allowed controlled heating of tumors, resulting in triggered release of DXR from TSL formulation remotely in an *in vivo* xenograft model. GNR + NIR was highly

effective in releasing the DXR from TSLs, as was evident from increased survival of animals receiving TSLs heated *via* GNRs. Interestingly, GNRs can also be used to increase the extent of passive accumulation of nanocarriers in the tumor region.[23,33] In this study, we demonstrated bioavailability of the chemotherapeutic from a nanocarrier is important and rapid drug release is more beneficial than the drug being slowly released from the nanocarrier over time. In the future, using GNRs to increase drug accumulation *via* hyperthermic blood vessel permeation at the tumor site and then using a second NIR pulse to disrupt the liposomes may significantly enhance the effects of chemotherapy.

MATERIALS AND METHODS

Liposome Preparation. 1,2-Distearoyl-*sn*-glycerophosphocholine (DSPC), 1,2-dimyristoyl-*sn*-glycero-3-phosphocholine (DMPC), and 1,2-distearoyl-*sn*-glycerophosphoethanolamine poly(ethylene glycol)$_{2000}$ (DSPE-PEG2000) were purchased from Genzyme Pharmaceuticals (Cambridge, MA). Liposomal nanocarriers were formed as described earlier.[34,35] Briefly, an *x*:97−*x*:3 ratio of DPPC:DSPC:PEG or a ratio 57−*x*:40−*x*:3 of DPPC:cholesterol:DSPE-PEG2000 or 57:3:30:3 of DPPC:DMPC:cholesterol:DSPE-PEG2000 was used to identify a thermosensitive formulation. A non-thermosensitive stealth liposomal formulation of DPPC:cholesterol:DSPE-PEG2000 in the ratio 57:40:3, respectively (NTSL), was used as a control in all *in vivo* studies. The lipid mixture was dissolved in 1 mL of ethanol at 60 °C. Liposome size was determined by dynamic light scattering (particle size analyzer, Brookhaven Instruments, Holtsville, NY). Liposomal nanocarriers were dialyzed (100 000 MW cutoff, Spectra/Por, Dominguez, CA) against a phosphate-buffered saline solution to establish an ammonium sulfate gradient for DXR loading.

Active Loading of Doxorubicin. Lipsomal nanocarriers were loaded with doxorubicin (Bedford Labratories, Bedford, OH) *via* the ammonium sulfate gradient as described before.[36] Briefly, liposomal nanocarriers and 5 mg/mL DXR solution in 0.9% saline were mixed at a ratio of 0.1 mg of DXR per 1 mg of phospholipid in the liposomal nanocarriers. The liposome/DXR suspension was heated at 45 °C for 30 min. The liposomal nanocarriers were then cooled immediately on ice and dialyzed in 100 000 MWCO membrane against phosphate-buffered slaine (PBS) to remove unencapsulated DXR. The formulations were sterilized by passing through a 0.2 μm filter. The final DXR concentration after dialysis was determined by lyses of the liposomal nanocarriers with 5% Triton X-100 and measurement of absorbance at 480 nm.

Liposomal Leak Studies. Liposomal DXR was diluted to a final concentration of 1 μg/mL in 50% FBS solution and heated in a circulating water bath at 37 °C for 24 h. The samples were placed in a water bath at 43 °C for 10 min in order to quantify drug release and then transferred back to the water bath at 37 °C. Twenty-four hours later all samples were analyzed for the amount of drug released. 100% release was the intensity after the addition of detergent Triton X-100, while 0% (no release) was the intensity measured for 50% FBS solution.[13] DXR intensity was measured at 485/590 excitation and emission wavelength in a spectrophotometer.

$$\%\text{release} = \frac{(\text{sample intensity})_T - (\text{sample intensity})_{25°C}}{(\text{max intensity})_{\text{lysed}} - (\text{sample intensity})_{25°C}}$$

where T = time.

***In Vitro* Cell Cytotoxicity Studies.** U-87 MG cells were purchased from ATCC and maintained as per ATCC recommendation. U87-MG glioma cells were seeded at a density of 2×10^4 cells per well of a 24-well plate and incubated for 48 h prior to incubation with liposomal nanocarriers. Forty-eight hours later, liposomal formulations were mixed with cell media to different doxorubicin concentrations and added immediately to the cells.

Cells were incubated with free DXR or liposomal DXR for 20 min at 37 or 43 °C and 5% CO_2 in a humidified environment. All wells were then incubated at 37 °C for an additional 4 h. Cells were then washed three times with fresh medium and reincubated for 72 h. The numbers of viable cells were determined with a water-soluble formazan-based assay, CCK-8 (Dojindo, Kumamoto, Japan).

Synthesis and PEGylation of Gold Nanorods. Gold nanorods were synthesized by the seed-mediated growth method.[37] Briefly, 2.50 mL of a 1.0 mM aqueous solution of $HAuCl_4$ (Sigma) was added to 5.0 mL of a 0.20 M aqueous solution of cetyltrimethylammonium bromide (CTAB, Sigma). The solution, at 25 °C, was then reduced with 600 uL of a 10 mM cold sodium borohydride solution (Sigma). The solution was allowed to react for several minutes, giving rise to a pale brown seed solution. Following preparation of the seed, 100 mL of a 1.0 mM $HAuCl_4$ solution and 4.50 mL of a 4.0 mM $AgNO_3$ (Fischer) solution were added to 100 mL of 0.20 M CTAB, after which 1.40 mL of 78.8 mM ascorbic acid (Sigma) was added and gently mixed to form a clear growth solution. The previously prepared seed solution (160 μL) was then added to the growth solution and left to react overnight. The GNR solutions were then purified by centrifugation at 14 000 rpm for 5 min, twice, and redispersed in deionized water. With this purification, any excess CTAB molecules were removed, and the GNRs were conjugated with mPEG-SH 5000 (Laysan Bio) at a concentration 10^4 times that of the GNRs. The solution was left to react overnight and centrifuged at 14 000 rpm for 5 min to remove any unbound PEG molecules. GNRs were redispersed in PBS (Mediatech) for use *in vivo*.

***In Vivo* Therapeutic Studies.** All animal studies were conducted under a protocol approved by the Institutional Animal Care and Use Committee (IACUC) at Georgia Institute of Technology. For the tumor model, the U87-MG human glioma cell line was used. A 100 μL aliquot containing 2×10^6 cells was subcutaneously injected using a 26-gauge needle into the right shoulder of 6−8 week old female nude mice (Charles River Laboratories International, Inc., Wilmington, MA). Caliper measurements were used to estimate tumor size, and the tumor volume was calculated as $V_{\text{tumor}} = ab^2/2$, where a and b are the maximum and minimum diameters, respectively.[38,39]

When tumors were about ~50−120 mm^3, animals were treated with a saline sham, TSL, and NTSL liposomal DXR i.v. injections (10, 5, and 2.5 mg/kg doxorubicin) *via* tail vein with or without GNRs. Equivalent volumes of 0.9% sterile saline solution were administered to animals receiving sham injections. Each treatment group consisted of ~6−9 animals. Tumor growth was allowed to progress until the tumors were 1.5 cm or showed signs of ulceration, at which point, interventional euthanasia was administered. Time of death was determined to be the day of euthanasia.

Heating via Gold Nanorods and Near-Infrared Radiation. Gold nanorods that accumulated in the tumor region due to EPR were heated by a NIR laser 48 h after treatment administration through the tail vein to heat the co-accumulated liposomes. Animals were anesthetized with 50, 10, and 1.67 mg/kg respectively of ketamine/xylazine/acepromazine. A 33-gauge hypodermic thermocouple (Omega), 10 mm long, was inserted into the tumor to measure the temperature rise at the tumor as described before.[21] Animals were then irradiated with NIR radiation at 810 nm, 0.5 W/cm^2 (808 nm diode laser, Power Technologies). The final experimental groups were (1) saline (n = 7), (2) saline + GNR + NIR (n = 7), (3) NTSL (n = 7), (4) NTSL + GNR + NIR (n = 6), (5) TSL + GNR (n = 6), (6) TSL + NIR (n = 6), and (7) TSL + GNR + NIR (n = 9).

***In Vivo* Apoptotic Imaging.** All animals used for *in vivo* fluorescence imaging were fed Teklad 2916 chlorophyll-free diet for 10 days prior to imaging to reduce autofluorescence.[40]

Tumor-bearing mice received 100 μL of Annexin-Vivo 72 h after treatment administration. All animals were imaged using IVIS Lumina (Caliper Life Sciences, Hopkinton, MA). Images were acquired using the appropriate filter set at 24 h after administering the imaging agent.

For analysis, images were loaded together to normalize all images to one color scale. A region of interest around the tumor was drawn, and the radiance flux was quantified for each time point. For comparison between groups, each animal's tumor volume was used to normalize the fluorescence intensity. Values obtained were then averaged for the respective group for statistical analysis.

Statistical Analysis. Means were determined for each variable in this study, and the resulting values from each experiment were subjected to an analysis of variance (ANOVA) with Tukey *posthoc* pairwise comparisons. Significance was determined using a 95% confidence test.

Acknowledgment. This work has been supported by funding from the National Science Foundation grant BES 0756567 to R.V.B. and a Georgia Cancer Coalition award to R.V.B. We would also like to acknowledge Dr. A. Annapragada, UT Houston, for technical discussions. The authors also acknowledge R. Trivedi, Georgia Tech, for help with the formulation and characterization of liposomes.

REFERENCES AND NOTES

1. Maeda, H.; Wu, J.; Sawa, T.; Matsumura, Y.; Hori, K. Tumor Vascular Permeability and the EPR Effect in Macromolecular Therapeutics: A Review. *J. Controlled Release* **2000**, *65*, 271–284.
2. Maeda, H. The Enhanced Permeability and Retention (EPR) Effect in Tumor Vasculature: The Key Role of Tumor-Selective Macromolecular Drug Targeting. *Adv Enzyme Regul.* **2001**, *41*, 189–207.
3. Woodle, M. C.; Lasic, D. D. Sterically Stabilized Liposomes. *Biochim. Biophys. Acta* **1992**, *1113*, 171–199.
4. Yuan, F.; Leunig, M.; Huang, S. K.; Berk, D. A.; Papahadjopoulos, D.; Jain, R. K. Microvascular Permeability and Interstitial Penetration of Sterically Stabilized (Stealth) Liposomes in a Human Tumor Xenograft. *Cancer Res.* **1994**, *54*, 3352–3356.
5. Andresen, T. L.; Jensen, S. S.; Jorgensen, K. Advanced Strategies in Liposomal Cancer Therapy: Problems and Prospects of Active and Tumor Specific Drug Release. *Prog. Lipid Res.* **2005**, *44*, 68–97.
6. Yatvin, M. B.; Kreutz, W.; Horwitz, B. A.; Shinitzky, M. pH-Sensitive Liposomes: Possible Clinical Implications. *Science* **1980**, *210*, 1253–1255.
7. Connor, J.; Yatvin, M. B.; Huang, L. pH-Sensitive Liposomes: Acid-Induced Liposome Fusion. *Proc. Natl. Acad. Sci. U. S. A.* **1984**, *81*, 1715–1718.
8. Wymer, N. J.; Gerasimov, O. V.; Thompson, D. H. Cascade Liposomal Triggering: Light-Induced Ca^{2+} Release from Diplasmenylcholine Liposomes Triggers PLA2-Catalyzed Hydrolysis and Contents Leakage from DPPC Liposomes. *Bioconjugate Chem.* **1998**, *9*, 305–308.
9. Mueller, A.; Bondurant, B.; O'Brien, D. F. Visible-Light-Stimulated Destabilization of PEG-Liposomes. *Macromolecules* **2000**, *33*, 4799–4804.
10. Meers, P. Enzyme-Activated Targeting of Liposomes. *Adv. Drug Delivery Rev.* **2001**, *53*, 265–272.
11. Davidsen, J.; Jorgensen, K.; Andresen, T. L.; Mouritsen, O. G. Secreted Phospholipase A(2) as a New Enzymatic Trigger Mechanism for Localised Liposomal Drug Release and Absorption in Diseased Tissue. *Biochim. Biophys. Acta* **2003**, *1609*, 95–101.
12. Yatvin, M. B.; Weinstein, J. N.; Dennis, W. H.; Blumenthal, R. Design of Liposomes for Enhanced Local Release of Drugs by Hyperthermia. *Science* **1978**, *202*, 1290–1293.
13. Gaber, M. H.; Hong, K.; Huang, S. K.; Papahadjopoulos, D. Thermosensitive Sterically Stabilized Liposomes: Formulation and *In vitro* studies on Mechanism of Doxorubicin Release by Bovine Serum and Human Plasma. *Pharm. Res.* **1995**, *12*, 1407–1416.
14. Kono, K.; Henmi, A.; Takagishi, T. Temperature-Controlled Interaction of Thermosensitive Polymer-Modified Cationic Liposomes with Negatively Charged Phospholipid Membranes. *Biochim. Biophys. Acta* **1999**, *1421*, 183–197.
15. Needham, D.; Anyarambhatla, G.; Kong, G.; Dewhirst, M. W. A New Temperature-Sensitive Liposome for Use with Mild Hyperthermia: Characterization and Testing in a Human Tumor Xenograft Model. *Cancer Res.* **2000**, *60*, 1197–1201.
16. Drummond, D. C.; Noble, C. O.; Hayes, M. E.; Park, J. W.; Kirpotin, D. B. Pharmacokinetics and *In vivo* Drug Release Rates in Liposomal Nanocarrier Development. *J. Pharm. Sci.* **2008**, *97*, 4696–4740.
17. Jain, P. K.; Huang, X.; El-Sayed, I. H.; El-Sayed, M. A. Noble Metals on the Nanoscale: Optical and Photothermal Properties and Some Applications in Imaging, Sensing, Biology, and Medicine. *Acc. Chem. Res.* **2008**, *41*, 1578–1586.
18. Huang, X.; Jain, P. K.; El-Sayed, I. H.; El-Sayed, M. A. Gold Nanoparticles: Interesting Optical Properties and Recent Applications in Cancer Diagnostics and Therapy. *Nanomedicine (London)* **2007**, *2*, 681–693.
19. El-Sayed, I.; Huang, X.; Macheret, F.; Humstoe, J. O.; Kramer, R.; El-Sayed, M. Effect of Plasmonic Gold Nanoparticles on Benign and Malignant Cellular Autofluorescence: A Novel Probe for Fluorescence Based Detection of Cancer. *Technol. Cancer Res. Treat.* **2007**, *6*, 403–412.
20. Huang, X.; Jain, P. K.; El-Sayed, I. H.; El-Sayed, M. A. Plasmonic Photothermal Therapy (PPTT) Using Gold Nanoparticles. *Lasers Med. Sci.* **2008**, *23*, 217–228.
21. Dickerson, E. B.; Dreaden, E. C.; Huang, X.; El-Sayed, I. H.; Chu, H.; Pushpanketh, S.; McDonald, J. F.; El-Sayed, M. A. Gold Nanorod Assisted Near-Infrared Plasmonic Photothermal Therapy (PPTT) of Squamous Cell Carcinoma in Mice. *Cancer Lett.* **2008**, *269*, 57–66.
22. Weissleder, R. A Clearer Vision for *In vivo* Imaging. *Nat. Biotechnol.* **2001**, *19*, 316–317.
23. Park, J. H.; von Maltzahn, G.; Xu, M. J.; Fogal, V.; Kotamraju, V. R.; Ruoslahti, E.; Bhatia, S. N.; Sailor, M. J. Cooperative Nanomaterial System to Sensitize, Target, and Treat Tumors. *Proc. Natl. Acad. Sci. U. S. A.* **2010**, *107*, 981–986.
24. Hunt, C. A. Liposomes Disposition *In vivo*. V. Liposome Stability in Plasma and Implications for Drug Carrier Function. *Biochim. Biophys. Acta* **1982**, *719*, 450–463.
25. Kiaris, H.; Schally, A. V.; Nagy, A.; Sun, B.; Szepeshazi, K.; Halmos, G. Regression of U-87 MG Human Glioblastomas in Nude Mice after Treatment with a Cytotoxic Somatostatin Analog AN-238. *Clin. Cancer Res.* **2000**, *6*, 709–717.
26. Gupta, B.; Torchilin, V. P. Monoclonal Antibody 2C5-Modified Doxorubicin-Loaded Liposomes with Significantly Enhanced Therapeutic Activity against Intracranial Human Brain U-87 MG Tumor Xenografts in Nude Mice. *Cancer Immunol Immunother.* **2007**, *56*, 1215–1223.
27. Paasonen, L.; Laaksonen, T.; Johans, C.; Yliperttula, M.; Kontturi, K.; Urtti, A. Gold Nanoparticles Enable Selective Light-Induced Contents Release from Liposomes. *J. Controlled Release* **2007**, *122*, 86–93.
28. Wu, G.; Mikhailovsky, A.; Khant, H. A.; Fu, C.; Chiu, W.; Zasadzinski, J. A. Remotely Triggered Liposome Release by Near-Infrared Light Absorption *via* Hollow Gold Nanoshells. *J. Am. Chem. Soc.* **2008**, *130*, 8175–8177.
29. Schutters, K.; Reutelingsperger, C. Phosphatidylserine Targeting for Diagnosis and Treatment of Human Diseases. *Apoptosis* **2010**, *15*, 1072–1082.
30. Ghoroghchian, P. P.; Therien, M. J.; Hammer, D. A. *In vivo* Fluorescence Imaging: A Personal Perspective. *Wiley Interdiscip. Rev. Nanomed. Nanobiotechnol.* **2009**, *1*, 156–167.
31. Graves, E. E.; Weissleder, R.; Ntziachristos, V. Fluorescence Molecular Imaging of Small Animal Tumor Models. *Curr. Mol. Med.* **2004**, *4*, 419–430.
32. Kocer, A. A Remote Controlled Valve in Lliposomes for Triggered Liposomal Release. *J. Liposome Res.* **2007**, *17*, 219–225.
33. Park, J. H.; von Maltzahn, G.; Ong, L. L.; Centrone, A.; Hatton, T. A.; Ruoslahti, E.; Bhatia, S. N.; Sailor, M. J. Cooperative

Nanoparticles for Tumor Detection and Photothermally Triggered Drug Delivery. *Adv. Mater.* **2010**, *22*, 880–885.
34. Saul, J. M.; Annapragada, A.; Natarajan, J. V.; Bellamkonda, R. V. Controlled Targeting of Liposomal Doxorubicin *via* the Folate Receptor *In vitro*. *J. Controlled Release* **2003**, *92*, 49–67.
35. Saul, J. M.; Annapragada, A. V.; Bellamkonda, R. V. A Dual-Ligand Approach for Enhancing Targeting Selectivity of Therapeutic Nanocarriers. *J. Controlled Release* **2006**, *114*, 277–287.
36. Bolotin, E. M.; Cohen, R.; Bar, L. K.; Emanuel, N.; Ninio, S.; Lasic, D. D.; Barenholz, Y. Ammonium Sulfate Gradients for Efficient and Stable Remote Loading of Amphipathic Weak Bases into Liposomes and Ligandoliposomes. *J. Liposome Res.* **1994**, *4*, 455–479.
37. Nikoobakht, B.; El-Sayed, M. A. Preparation and Growth Mechanism of Gold Nanorods (NRs) Using Seed-Mediated Growth Method. *Chem. Mater.* **2003**, *15*, 1957–1962.
38. Tomayko, M. M.; Reynolds, C. P. Determination of Subcutaneous Tumor Size in Athymic (Nude) Mice. *Cancer Chemother. Pharmacol.* **1989**, *24*, 148–154.
39. Euhus, D. M.; Hudd, C.; LaRegina, M. C.; Johnson, F. E. Tumor Measurement in the Nude Mouse. *J. Surg. Oncol.* **1986**, *31*, 229–234.
40. Troy, T.; Jekic-McMullen, D.; Sambucetti, L.; Rice, B. Quantitative Comparison of the Sensitivity of Detection of Fluorescent and Bioluminescent Reporters in Animal Models. *Mol. Imaging* **2004**, *3*, 9–23.